

Numerical Simulation of Flow in Rectangular Duct with Different Obstruction Heights

Lect. Kadhum Audaa Jehhef
Department of Equipment and Machine
Institute of Technology
Middle Technical University
Email: kadhum.audaa@yahoo.com

ABSTRACT

In this study, a simulation model inside a channel of rectangular section with high of (0.16 m) containing two rectangular obstruction plates were aligned variable heights normal to the direction of flow, use six model of the obstructions height of (0.059, 0.066, 0.073, 0.08 and 0.087 m) were compared with the flow behavior of the same duct without obstructions. To predict the velocity profile, pressure distribution, pressure coefficient and turbulence kinetic energy flow of air, the differential equations which describe the flow were approximated by the finite volumes method for two dimensional, by using commercial software package (FLUENT) with standard of k-ε model two dimensions turbulence flow. The obtained results show that the velocity and the turbulence kinetic energy increase with increasing the obstructions height perpendicular to the flow direction. Streamlines contours used to show mixing of averaged flow-field in one pitch length. The streamlines helped to distinguish between important separated regions of the flow as well. Compared the first model of height of obstruction (0.059 m) with the fifth model of the obstruction of height (0.087 m) it is obtained an increasing in velocity about of (71 %) at the first obstruction and an increasing about (47 %) at the second obstruction. The data obtained by simulation are matching with previous the literature value.

Keywords: turbulent flow, obstructions plates, air duct.

محاكاة عددية للجريان داخل مجرى مزود بعوارض ذات ارتفاعات متغيرة

م.د. كاظم عودة جحف

قسم المكنان والمعدات

معهد تكنولوجيا- بغداد

الجامعة التقنية الوسطى

الخلاصة

تتناول الدراسة الحالية استخدام نموذج محاكاة داخل مجرى مستطيل المقطع بارتفاع (0.16 م) يحتوي على صفيحتان اعترضيتان باتجاه معاكس ذات ارتفاع متغير عمودي على الجريان داخل المجرى , وتم استخدام ست نماذج لارتفاعات الصفيحة المعترضة هي: (0.059, 0.066, 0.073, 0.08 و 0.087 m) وقورنت النتائج مع نموذج اخر لنفس ظروف الجريان ولكن بدون معترضات. من اجل تخمين سلوك كلامن توزيع السرعة و الضغط و معامل الضغط والطاقة الحركية للجريان الاضطرابي للهواء , تم استخدام طريقة الحجم المحددة لحل المعادلات التفاضلية التي تصف حركة المائع وذلك لبعدين, واستخدام البرمجيات الحاسوبية مثل برنامج (FLUENT) وهذا البرنامج مدعوم بنموذج حسابي k-ε model خاص بالجريان الاضطرابي , النتائج التي تم الحصول عليها تظهر ان قيم السرعة والطاقة الحركية للجريان الاضطرابي تزداد بزيادة ارتفاع المعترضات العمودية على خطوط الجريان وتستخدم لملاحظة عملية الخلط الحاصلة في المجال في منطقة الخطوة المحصورة بين المعترضات. خطوط الجريان تساعد ايضا على التمييز بين المناطق المنفصلة داخل الجريان. وبمقارنة النموذج الاول ذو ارتفاع (0.059 m) مع النموذج الخامس ذو ارتفاع المعترض (0.087 m) نحصل على نسبة زيادة بقيمة السرعة بنحو (71 %) عند المعترض الاول وبنسبة (47%) عند المعترض الثاني وقد اظهرت النتائج النظرية تطابقا ملموسا مع نتائج البحوث السابقة.

الكلمات الرئيسية: الجريان الاضطرابي , الصفائح المعترضة, المجاري الهوائية.

1. INTRODUCTION

The flow in ducts with plates represents a topic of paramount industrial interest. This geometry is representing the internal channels of turbine blades for cooling. The understanding of this flow is then very important for the optimization of cooling process. The phenomenon of flow separation in ducts with segmented baffles or obstructions has many engineering applications, for example, shell-and-tube heat exchangers with segmented obstructions, labyrinth shaft seals, laser curtain seals, air-cooled solar collectors, and internally cooled turbine blade. One of the techniques used to enhance the convective heat transfer in a smooth channel is to place obstructions on the channel walls in-line or staggered arrangement. Turbulent flow and heat through ducts roughened with both attached and detached ribs has the topic of many experimental and numerical studies. However, the researches relating the detached ribs are few. , **Lio and Chen, 1993.** and , **Rau et al, 1988** studied the turbulent flow in channels with attached ribs. The main objectives of these studies were to obtain the heat transfer characteristics and friction factor. , **Goax and Sunden, 2001** by using oblique and shaped attached ribs to the duct wall. These studies conducted that the resulting secondary flow from the ribs increase the fluid mixing between the core region and near wall region.

Investigation of characteristics of the turbulent flow and heat transfer inside the periodic cell formed between segmented baffles staggered in a rectangular duct was studied by , **Habib et al., 1994.** To show that the pressure drop increases as the baffle height does. The heat flux was uniform in both upper and lower walls. The experiments focused on the influence of Reynolds number and baffle height on the local and global heat transfer coefficients, and pressure drop measurements. Large recirculation regions and velocity gradients were observed behind the baffles. Pressure drop increases more rapidly than the heat transfer coefficient with the Reynolds number.

Experimental investigation of complex flow, turbulent flow along an external corner has been conducted by , **Moinuddin et.al, 2004.** and , **Luo et.al, 2003.** They studied the fully developed turbulent flow in an air-cooled horizontal equilateral triangular duct fabricated on its internal surfaces with uniformly spaced square ribs. Five different rib sizes of 5 mm, 6 mm, 7 mm, 7.9 mm and 9 mm were considered. Both the ducts and the ribs were fabricated with duralumin. The experimental results showed that the pressure drop along the triangular duct, increased almost linearly with the rib size. The developed equations were valid for a wide range of Reynolds numbers $4,000 < Re_D < 23,000$.

Zilwa et al., 1998, studied laminar and turbulent flows through plane sudden expansions. Turbulent flow simulations using k-ε models showed to be very reliable when compared to experimental results. Measurements using LDA technique in the turbulent flow in a duct with several baffle plates were performed by , **Berner et al., 1984** with the purpose of determining the number of baffles necessary for obtaining a periodic boundary condition and the dependence on Reynolds number and the geometry. Results showed that with a Reynolds number of 5.17×10^3 four baffles were necessary for obtaining a periodic boundary condition. By increasing the Reynolds number to 1.02×10^4 a periodic boundary condition was obtained with three baffles.

Li and Kottke, 1998 studied heat transfer and pressure drop in simulating models of shell-and-tube heat exchangers. Two variable parameters used in the experimental work the Reynolds



number and the distance between the baffles. Results demonstrated that for a constant value of the Reynolds number, an increasing the distance between the baffles increases the heat exchange coefficient and the pressure drop.

A numerical analysis presented by , **Jin-Xing et al., 2006**, The baffle heat exchanger can slightly enhance the shell side heat transfer coefficient with the significant reduction of pressure loss due to the shell side fluid flowing longitudinally through tube bundle, which leads to the reduction of the manufacture and running cost and in some cases to the dimensions reduction of the heat exchangers. The numerical results showed that the baffles placed vertically and horizontally in the unit duct continue to shear and comminute the streamline flow when the fluid crosses over the baffles, change the fluid flow directions.

The finite volume commercial code Fluent 6.1 was used by **Márton, 2005** to compute the flow-field inside a square section duct with square section ribs mounted on one side perpendicularly to the flow direction successively, the Reynolds number was 40000 based on the hydraulic diameter (D_h). The rib height (h) to hydraulic diameter ratio was 0.3, and the pitch (p) to rib ratio was 10. Computation was carried out in one pitch length using periodic boundary condition in streamwise direction. The same flow configuration was investigated previously at the Von Kármán Institute for fluid dynamics by experimental techniques it is compares with the results with the PIV measurement of , **Casarsa et al. 2002**. The comparison in the symmetry plane of the duct ($Z/h=0$) was shown because this seemed to be the most characteristic for the main features of the flow.

,**Moosavy and Hooman, 2008** performed study about laminar heat and fluid flow in the entrance region of a two dimensional horizontal channel with isothermal walls and staggered baffles. The computations were based on the finite volume method and the SIMPLER algorithm. Data for heat and fluid flow as well as pressure drop were presented for the Reynolds numbers ranging from 50 to 500 and baffle heights between 0 and 0.75. The results were reported for the thermal entrance region with sixteen baffles. This relatively large number of baffles allowed to think of working media except air and water so that the Prandtl number may vary from 0.7 to 70. While most of the work available in the literature showed the effects of Reynolds number on the hydrodynamic development of flow that not only the Reynolds number but also the Prandtl number affects the precise location of the periodically fully developed region similar to the case of smooth channel. It is not surprising when one observes that most of the previous articles are concentrated on moderate Prandtl numbers compared.

2. OBJECTIVES

From previous works review there are no attention on the height of the obstruction or baffle in the flow field in the air ducts. The present paper will present the method and the results of a numerical simulation of rectangular section containing two rectangular obstruction plates were aligned variable height normal to the main flow direction, using the commercial solver (FLUENT version 6.3.26). A secondary objective is to show the differences between the developed flow fields in the duct containing two rectangular obstruction plates with the duct without rectangular obstruction plates.

3. MATHEMATICAL FORMULATION

In Reynolds averaged approach to turbulence, all of the unsteadiness is regarded as a part of the turbulence. Applying the Reynolds decomposition, the nonlinearity of the Navier-Stokes equations gives a rise to terms that must be modeled. In a statistically steady flow, every variable can be written as a sum of an average and a fluctuation, **Mushatet and Mehdi, 2008**. In this paper use the following assumption:

1. Steady turbulent flow.
2. Two dimensional flow constant properties.
3. No edge effects.
4. No buoyancy effects.
5. Fully developed flow.
6. No heat generation.
7. Negligible axial diffusion.
8. No slip and impermeability boundary conditions are imposed at the walls.

This must be large enough to eliminate the effects of the fluctuations. The averaged equations of continuity and momentum can be written in the following form, **Vass P., 2005**.

$$\partial_j(u_j) = 0 \tag{1}$$

$$\partial_t(u_i) + \partial_j((u_j)(u_i)) = \partial_i(p) + \partial_j\left(\frac{1}{Re_b} \partial_j(u_i)\right) + (g_i) - \partial_j \tau_{ij}^R \tag{2}$$

$$\tau_{ij}^R = (u_i' u_j') \tag{3}$$

Balance equations for the kinetic energy (k) and its dissipation rate (ε) for the model are, **Mushatet and Mehdi, 2008**:

$$\rho \left(\frac{\partial k}{\partial t} + U_j \frac{\partial k}{\partial X_j} \right) = \frac{\partial}{\partial X_j} \left[\left(\mu + \frac{\mu_t}{\sigma_k} \right) \frac{\partial k}{\partial X_j} \right] + G_k - \rho \epsilon \tag{4}$$

$$\rho \left(\frac{\partial \epsilon}{\partial t} + U_j \frac{\partial \epsilon}{\partial X_j} \right) = \frac{\partial}{\partial X_j} \left[\left(\mu + \frac{\mu_t}{\sigma_\epsilon} \right) \frac{\partial \epsilon}{\partial X_j} \right] + G_{1\epsilon} \frac{\epsilon}{k} G_k - G_{2\epsilon} \rho \frac{\epsilon}{k} \tag{5}$$

Where τ_{ij}^R is the mean stress tensor or Reynolds stress tensor, called "standard k-ε" model is a semi-empirical one, based on the conservation equation of the kinetic energy (k) and its dissipation rate (ε). The basis of the model is Boussinesq's hypothesis, that the Reynolds stresses $-\rho \overline{U_i' U_j'}$ are proportional to the strain rate of the mean flow, by means of the eddy viscosity concept:

$$\mu_t = \rho C_\mu \frac{k^2}{\epsilon}$$

G_k represents the production rate of the kinetic energy due to the energy transfer from the mean flow to turbulence, given by

$$G_k = -\rho \overline{U_i' U_j'} \frac{\partial U_j}{\partial X_i} \tag{6}$$

And can represent the G_k by:



$$G_k = \mu_t S^2$$

Where S is the modulus of the mean strain tensor, given by

$$S = \sqrt{2S_{ij}S_{ij}} \tag{7}$$

And the strain tensor is

$$S_{ij} = \frac{1}{2} \left(\frac{\partial \bar{U}_i}{\partial X_j} + \frac{\partial \bar{U}_j}{\partial X_i} \right) \tag{8}$$

Considering the effects of the wall for the standard k-ε model, **Launder and Spalding 1972**, a “law of the wall” for the mean velocity distribution is given by

$$U^* = \frac{1}{\kappa} \ln(Ey^*) \tag{9}$$

Where y* is the dimensionless distance to the wall is given by:

$$y^* = \frac{\rho C_\mu^{1/4} k_P^{1/2} y_P}{\mu} \tag{10}$$

κ= Von Kármán constant (= 0.42)

E = empirical constant (= 9,81)

U_P = time average velocity at position P

P_k = kinetic energy of turbulence at position P

P_y = distance from position P to the wall

One of the most widely spread models is the standard k-ε model proposed by **Launder and Spalding 1972**. This model implies two transport equations turbulent kinetic energy (k, m²/s²) and the dissipation of turbulent kinetic energy (ε, m²/s³) to remedy the large steep gradients near the walls of the duct and the baffle plates; wall function approximation used by **Versteeg, 1995** is adopted the model coefficients are (σ_k; σ_ε; C_{1ε}; C_{2ε}; C_μ) = (1.0, 1.3, 1.44, 1.92, 0.09) respectively.

3.1 Computational Model and Boundary Conditions

The present paper performs the turbulent flow in a rectangular cross section duct were two obstructions were placed, so as to simulate the conditions found in shell-and-tube heat exchangers, where flow and pressure distribution need to be known. The physical domain is shown in **Fig.1** the flow geometry under consideration and the boundary conditions used in this paper (top and lower) walls and (top and lower) plates considered as a wall boundary conditions zero velocity conditions (at y=0 and y=H →U=0) and the inlet velocity at the entrance of the duct (at y=H/2→U=U_o) the fluid enters at an inlet velocity, U_{in}=U_o=(8 m/s) (reference velocity), where the discharge of the duct exposure to the atmospheric pressure (P =P_{atm}). The total length of the duct is equal to 0.554 m where obstructions plate with variable height about (0.059, 0.066, 0.073, 0.080, and 0.087) toward the flow which is not sufficient for the flow development.

Therefore, no influence will result from the side walls, so that the flow can be considered as being two-dimensional. The Reynolds number was Re = 1.44×10⁵ based on duct hydraulic diameter (D_H) such that:

$$Re = \frac{\rho D_H U_o}{\mu} \tag{11}$$

Where D_H is the hydraulic diameter of the channel equal to 0.275 m determine by:

$$D_H = \frac{4A}{P} = \frac{4(H*W)}{2(H+W)} \quad (12)$$

Kinetic energy of turbulence and dissipation rates are prescribed, following, as

$$k_o = 0.005U_o^2$$

$$\varepsilon_o = \frac{k_o^{1.5}}{\lambda H} \quad \lambda = 0.005$$

Where $U_{inlet} = U_o$ the inlet velocity of air, for the upper and lower walls it is imposed

$$\frac{\partial k}{\partial n} = 0$$

3.2 GEOMETRY AND GRID ARRANGEMENT

The geometry and the grid were generated using GAMBIT® the preprocessing module of the FLUENT code. The geometry consist of a rectangular duct height 0.16 m and length of 0.554 m, the first obstructions plate is located 0.218 m from inlet section at the top plate and the second with the distance of 0.142 from the first one at lower plate, using a two-dimensional formulation with the SIMPLEX-algorithm [18] built and tested with the (Fluent 6.6.26) (©Fluent Inc., 2000). The mesh was generated by the pre-processor software (Gambit 2.3.16). This code is based on hybrid scheme. Due to this strong inherent coupling and non-linearity inherent in these equations, relaxation factors are needed to ensure convergence. The relaxation factors used for velocity components, pressure, temperature and turbulence quantities are 0.5, 1, 0.7 and 0.7 respectively. The mesh was refined at all solid boundaries; however these relaxation factors have been adjusted for each case studied to accelerate the convergence criterion defined as the relative deference of every dependent variable between iteration steps. In order to ensure that the numerical computations are not significantly affected by the mesh, by using the multi zone meshing generated the Map mesh with interval account of (180 × 60) and 10131 nodes in the geometry. With made a clustered zone near the obstruction wall by interval size about 1.05 the that near the baffle plate near the solid boundary to resolve velocity and pressure gradient as shown in **Fig. 2** additional refinements were performed, considering the geometry and features of the numerical solution of the problem. **Fig. 3** presents an example of the mesh used near the tip of a obstruction plate in the presence of flow separation. This refinement was necessary to resolve the velocity and pressure gradients in that region. Necessary fluid exit, entry and wall boundary conditions were given before numerical simulation.

The solution control and the initialization of the solution have to be given before the iteration starts to reach the converges. The solution controls like the pressure velocity coupling and the discrimination of the different variables. The SIMPLE scheme for the pressure velocity coupling is used and the second discrimination is used for the momentum and the standard scheme is used for the pressure. Besides, in the channel outlet it is prescribed the atmospheric pressure.

4. RESULTS AND DISCUSSION

Four position were taken in this study to presented all the profiles in the two dimension of the test duct in the x-axis of the duct there are the ($x = 0$ m, $x = 0.218$ m, $x = 0.336$ m, $x = 0.554$ m) represented the entrance, first obstructions position, second obstructions position, and the outlet the duct. This technique used in all models of the study with variable length the baffles of (0.059, 0.066, 0.073, 0.08 and 0.087) respectively. **Figs. (4 to 8)** include the numerical results of mean velocity profiles for these positions measured downstream of the entrance. These positions are located upstream of the entrance, located at an $x = 0.218$ m and $x = 0.336$ m from the entrance. Velocity values are obtained from the fluent result for the models of (0.059, 0.066, 0.073, 0.08 and 0.087 m). For the one model it is show the entrance velocity kept constant with increasing y-value (the height of the duct) at the value of (8 m/s) with increasing x-value to the (0.218 m) were at the position of the first obstruction observe increasing the values of the velocity at the range of height of the duct of (0 to 0.06 m) from the lower wall to the centerline of the duct.

But at the x-axis of (0.336 m) show a high increasing in the velocity values at the range of high of (0 to 0.16) from the lower to top wall but with values less than that the velocity at the outlet of the duct at ($x=0.554$ m). The effect of increasing the obstruction length on the velocity magnitude in the duct, increasing the velocity of the flow approaching the passage under the obstruction and the increasing the obstruction length leading to increase the velocity magnitude shown clearly at the second obstruction plate where show that the value of the velocity approximately about (24.4 m/s) when used the third model (0.073 m height obstruction plate) with compared with second model (0.066 m height obstruction plate) obtained outlet velocity about (28.8 m/s).

The presence of the baffle plates influences not only the velocity field but also the pressure distribution in the whole domain investigated. To represent the pressure field in dimensionless form, a pressure coefficient is defined a **Demartini L. C. et al., 2004**

$$C_p = \frac{(p - p_{atm})}{\frac{\rho U_0^2}{2}} \quad (11)$$

Where p is the static pressure and p_{atm} is the atmospheric pressure. For the comparison of numeric with experimental results of C_p , the pressure p is the measured wall pressure or the calculated pressure. **Figs.9** show the numerical results of pressure coefficients at positions ($x = 0.218$ m and $x = 0.336$ m) respectively compared with value of the entrance and the out let of the duct the figure show that the pressure coefficients remain constant at the entrance and the out let of the duct. The pressure coefficients increasing at the first obstruction (from 0 to 654) and at the second obstruction decreasing from (702 to 321). **Fig.9 and 10** represented numerical results comparison of the values of pressure coefficients visa versa the height of the duct at the sections of ($x = 0.218$ m) and ($x = 0.336$ m) respectively shown increasing the pressure coefficients values with increasing height obstruction plate and The lower pressure values near the tip of the baffles are due to the high velocities in that region.

The turbulence kinetic energy very important indicator to the intensity of the turbulent flow in the duct, **Figs. 11 to 15** show the turbulence kinetic energy of the first obstruction plate, the second obstruction plate, the inlet section and the outlet section of the duct, for all heights of the

obstruction plate of (0.059, 0.066, 0.073, 0.08 and 0.087 m). For example at the case of height (0.059 m) of the obstruction the turbulence kinetic energy increasing from (41.2 to 68.3 m^2/s^2) from section of the first to the second obstruction plate, with compared with the case of obstruction height of (0.087 m) obtain increasing about (71 %) at the first obstruction and increasing about (47 %) at the second obstruction when used the case of height of obstruction of (0.059 m).

The effect of obstructions plates on the recirculation regions and the structures of the flow is depicted in **Figs 16 to 18** for case of with obstructions plates (the case of height obstructions of (0.059 m)) and without obstructions plates and **Figs 19 to 21** for case of demonstrate the comparison between the case of duct with and without the obstructions plate on the flow characteristics. As the figure shows the recirculation zones are significantly increase with the use the plate obstructions, these figures give a detail description of stream function and streamlines and axial stream wise velocity contours. The flow separates downstream each obstruction plate forming large recirculation zone where the region behind the obstruction plate works as a sudden expansion. The recirculation zoon seems to be larger at the first obstruction plate. The first obstruction plate accelerate the flow along with separated zone creates a significant pressure loss. In the downstream of the obstruction plates, the mixing promoted by turbulence and the separation zone is decreased. The separation zone is larger and the flow is faster in the distance between the obstruction plates, the recirculation zone behind the first obstruction plates is less compared with the other zones in the stream wise direction because the acceleration of the flow is larger behind the first obstruction plate and that leads to increase in separation zone in the next obstruction plate.

The effect of increasing the height obstructions plates on the recirculation regions and the structures of the flow is depicted in **Figs 22** illustrates the effect of the obstructions height on velocity field distribution and the streamlines function contours for the behavior of the fluid inside the duct. Flow is from left to right in duct of the case of height obstructions of (0.087 m) compared with the case of height obstructions of (0.059 m) compared with the **Fig. 19** (the case of height obstructions of (0.059 m)) the numerical results show very low velocity values adjacent to the obstructions plates. In the regions downstream of both obstructions plates, recirculation cells with very low velocity values are observed. In the regions between the tip of the baffle plates and the channel walls, the velocity is increased. Due to the changes in the flow direction produced by the baffle plates, the highest velocity values appear near the upper channel wall with an acceleration process that starts just after the second obstructions plates. And **Fig. 23** the case of height obstructions of (0.087 m) has shown the contours of streamline function distribution compared with the **Fig. 20** (the case of height obstructions of (0.059 m)) of streamline function distribution streamline values in (kg/sec) observe generate an circulation motion of the fluid with high value of stream line behind the obstruction, this circulation motion of the fluid increasing with increase the obstruction height. Compression the present numerical result with the numerical and experimental results of the (Demartini et. al., 2004) used baffle height ($H=0.08$ m) showed in the **Fig. 24 and 25** dimensionless velocity profiles the first and second obstruction plate the present models for the first ($H=0.059$) gives low velocity magnitude and fifth model ($H=0.087$) gives high velocity magnitude compare with the model used by (Demartini et. al., 2004) because the velocity increase with increase the obstruction height.

5. CONCLUSIONS

Numerical calculations are presented for turbulent fluid flow in a rectangular duct with segmented obstructions plates that are staggeringly arranged on both top and bottom walls of the duct. The results are reported for fixed baffle spacing and different values height obstructions plates. It was observed increase in the velocity magnitude with increasing the obstruction length where at the second obstruction plate where show that the value of the velocity increasing approximately about (16 %) when used the third model (0.073 m height obstruction plate) with compared with second model (0.066 m height obstruction plate). And the pressure coefficients increasing at the first obstruction (from 0 to 654) and at the second obstruction decreasing from (702 to 321) at ($x = 0.218$ m) to ($x = 0.336$ m). the case of height (0.059 m) of the obstruction the turbulence kinetic energy compared with the case of obstruction height of (0.087 m) obtain increasing about (71 %) at the first obstruction and increasing about (47 %) at the second obstruction when used the case of height of obstruction of (0.059 m), where observe generate an circulation motion of the fluid with high value of stream line behind the obstruction, this circulation motion of the fluid increasing with increase the obstruction height.

REFERENCES

- Berner, C., Durst, F. and Mcelligot, D. M., (1984), "*Flow around baffles*", Journal of Heat Transfer, vol. 106, pp. 743-749.
- Casarsa, L. Çakan, M. and Arts, T. (2002), "*Characterization of the velocity and heat transfer fields in an internal cooling channel with high blockage ratio*". Proceedings of ASME Turbo Expo. Amsterdam, the Netherlands.
- De Zilwa, S .R N., Khezzar, L. K. and Whitelaw, J. H., (1998). "*Flows through plane sudden-expansions*", International Journal for Numerical Methods in Fluids, nr. 32, pp. 313-329.
- Demartini L. C., Vielmo H. A. and Möller S. V., (2004). "*Numerical and experimental analysis of the turbulent flow through a channel with baffle plates*" J. of the Braz. Soc. of Mech. Sci. & Eng. Vol. xxvi, No. 2 pp. 153- 159.
- Goax, X. and Sunden, B. (2001). "*Heat transfer and pressure drop measurements in rib-roughened rectangular ducts*", experimental thermal and fluid science, 24.
- Habib, M.A., Mobarak, A.M., Sallak, M.A., Hadi, E.A. and Affify, R.I. (2004). "*Experimental investigation of heat transfer and flow over baffles of different height*" ASME- mechanical eng, Journal of Heat Transfer; pp: 363-368; Vol: 116 King Fahd university of Petroleum & Minerals.



- Jin-Xing W.U., Dong, L.I.U. and Min-Shan W.E.I. (2006). " *Simulation on the unit duct in the shell side of the ROD baffle heat exchanger*" Journal of Shanghai University (English Edition), No.4, pp. 362 - 365.
- Launder, B. E. and Spalding, D. B., (1974). " *The numerical computation of turbulent flows*", Computer Methods in Applied Mechanics and Engineering, vol. 3, pp. 269-289.
- Launder, B.E. and Spalding, D.B., (1972). " *Lectures in mathematical model of turbulence*", Academic Press, London and New York.
- Li, H. and Kottke, V., (1998). " *Effect of baffle spacing on pressure drop and local heat transfer in staggered tube arrangement*", International Journal of Heat and Mass Transfer, vol. 41, No. 10, pp. 1303-1311.
- Lio, T.M, Hwang, G.G. and Chen, S.H. (1993). " *Simulation and measurements of enhanced turbulent heat transfer in channels with periodic ribs on one principal wall*", international Journal of heat mass transfer, 36, 507-507.
- Máté Márton Lohász, Patrick Rambaud and Carlo Benociles, (2002). " *Computation of Flow in A Ribbed Square Duct Using Fluent and Comparison To PIV*" on kármán institute for fluid dynamics, Belgium department of fluid mechanics, Budapest University of Technology and Economics, Budapest, Hungary.
- Moinuddin, K. A. M., Joubert, P. N. and Chong, M. S., (2004). " *Experimental investigation of turbulence driven secondary motion on a streamwise external corner*". J. Fluid Mech., 511, pp. 1–23.
- Moinuddin, K. A. M., Joubert, P. N., Chong, M. S. and Hafez, S. (2003), " *Experimental investigation of turbulent boundary layer developing along a streamwise external corner*", Thermal and Fluid Science, 27(5), pp. 599–609.
- Moosavy, S.S. and Hooman, K., (2008), " *Forced convection in entrance region of a channel with staggered baffles*", Nuclear Research Center for Agriculture and Medicine, Karaj, Iran Mechanical Engineering Department, Bushehr Faculty of Engineering, Persian Gulf University, Bushehr, Iran.
- Mushatetl K.S., and Mehdi G.S, (2008), " *Analysis of turbulent flow in a duct roughened with attached and detached ribs*" Mechanical Engineering Department, College of Engineering, University of Thiqr, Iraq.
- Rau, G., Cakan, M., Moeller, D. and Arts, T. (1988). " *The effect of periodic ribs on the local aerodynamics and heat transfer performance of a straight cooling channel*", ASME Journal of turbo machinery, 120, pp. 368-375.



- Van Doormaal J. P. and Raithby G. D., (1985). “*Enhancements of the SIMPLE method for predicting incompressible fluid flow*”, Numerical Heat Transfer, vol. 7, pp 147-163.
- Vass P., (2005). "*Large eddy simulation of a ribbed duct flow with fluent effect of rib inclination*" University of Catholique de Louvain, Diploma thesis, May.
- Versteeg, H. and Meer, W., (1995). "*An introduction of computational fluid dynamics*", Hemisphere Publishing Corporation, United State of America.

NOMENCLATURE

E	empirical constant
H	duct height, m
h	obstruction height, m
i, j	tensor notation.
k	turbulent kinetic energy, m^2/s^2
k_P	kinetic energy of turbulence at position P, m^2/s^2
P	pressure, Pa
p	obstruction pitch, m
p_{atm}	atmospheric pressure, bar
Re	Reynolds number
S	modulus of the mean strain tensor
U_{in}	inlet velocity, m/s
U_P	time average velocity at position, m/s
$-\rho \overline{U'_i U'_j}$	Reynolds stresses N/m^2
$\overline{U'_i}$ and $\overline{U'_j}$	mean velocity components, m/s
W	Width of the duct, m
X_i and X_j	directions.
y_P	distance from position P to the wall, m

Greek symbols:

μ	molecular viscosity, Pa/s
ν_t	eddy viscosity, m^2/s^2
ρ	air density, kg/m^3
δ_{ij}	the Kroenecker Delta
κ	Von Karman constant
ε	dissipation rate, m^2/s^3
k	kinetic energy, m^2/s^2
σ_k	turbulent Prandtl number for turbulence
σ_c	turbulent Prandle number for dissipation of turbulence.

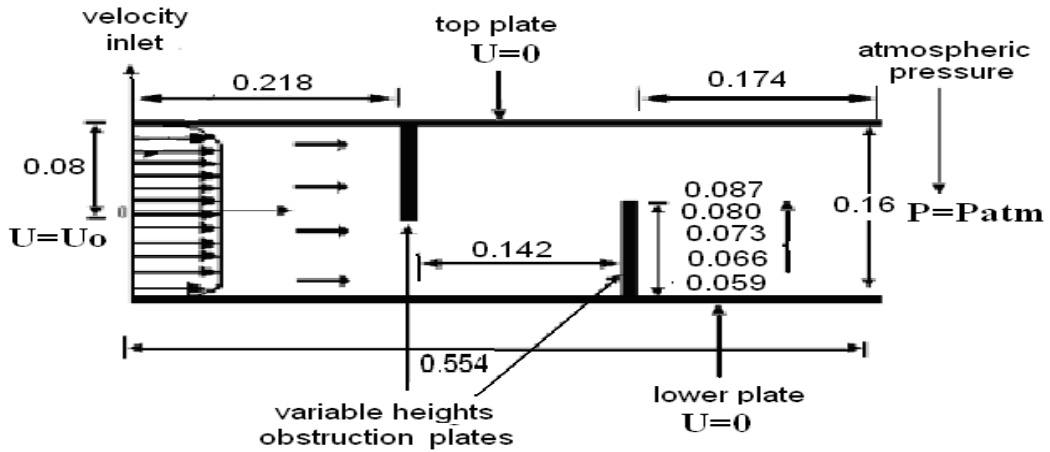


Figure 1. Detail of the duct with the obstruction plates and boundary conditions (dimensions in m).

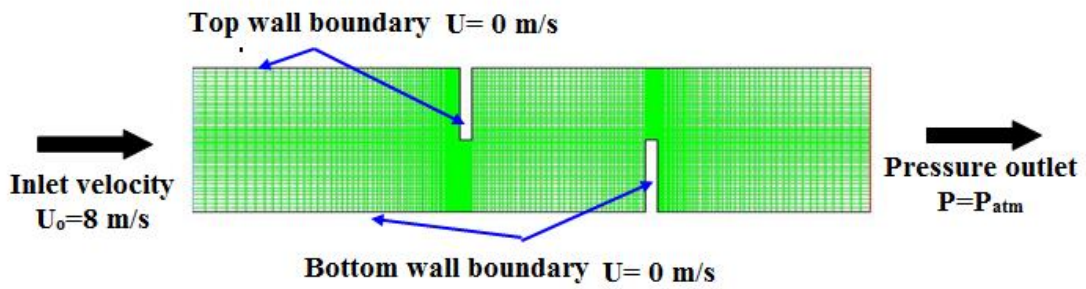


Figure 2. Mesh generated on the tip of the first obstruction plate with refinements and the boundary conditions.

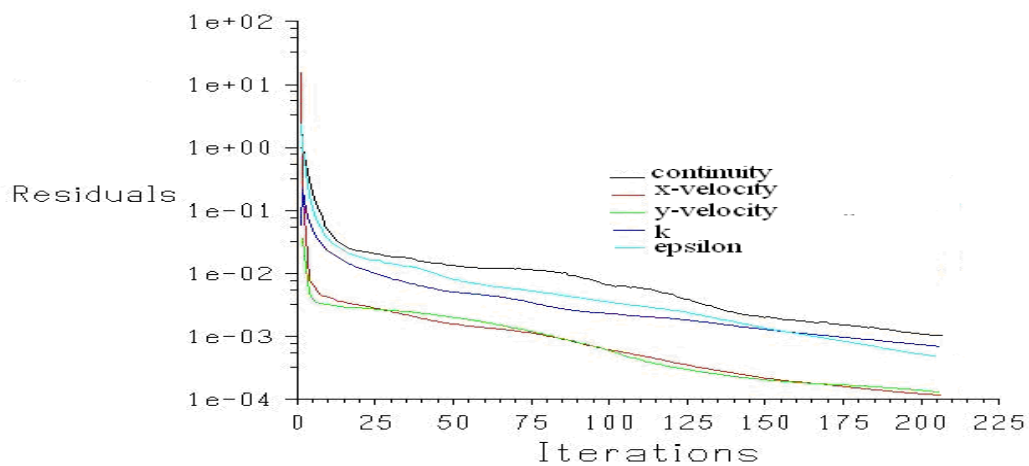


Figure 3. Resolution and iterations for the simulations runs

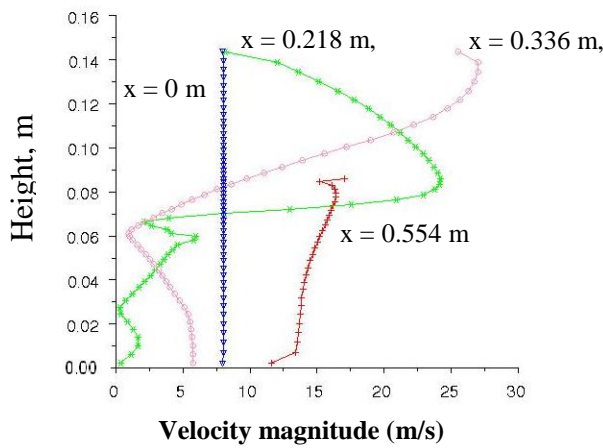


Figure 4. Velocity profiles at the first plate, second plate, inlet section and outlet section of the duct with obstruction height 0.059 m.

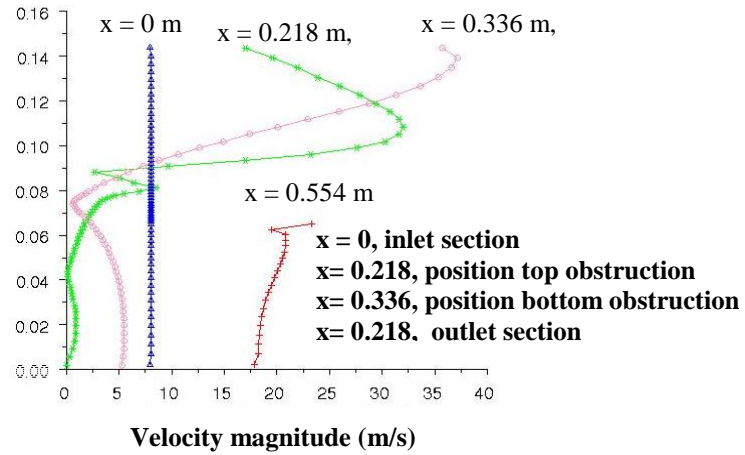


Figure 7. Velocity profiles at the first plate, second plate, inlet section and outlet section of the duct with obstruction height 0.080 m.

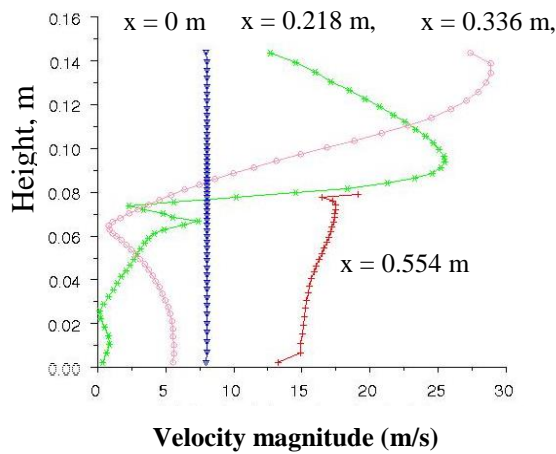


Figure 5. Velocity profiles at the first plate, second plate, inlet section and outlet section of the duct with obstruction height 0.066 m.

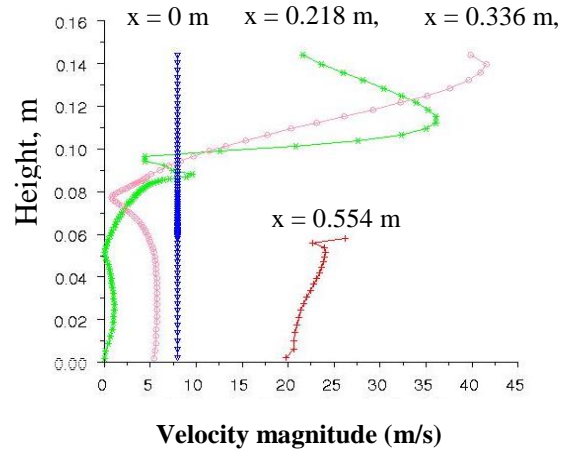


Figure 6. Velocity profiles at the first plate, second plate, inlet section and outlet section of the duct with obstruction height 0.087 m.

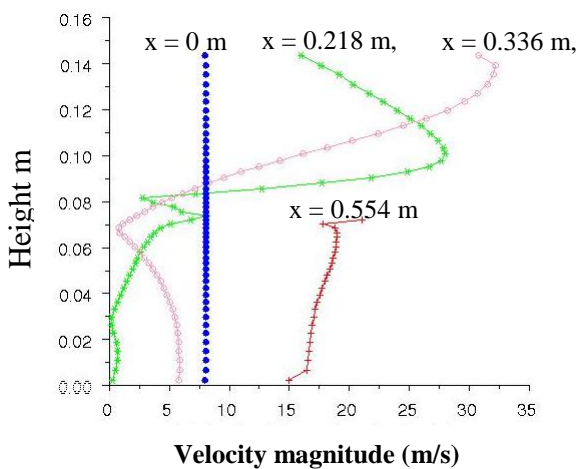


Figure 6. Velocity profiles at the first plate, second plate, inlet section and outlet section of the duct with obstruction height 0.073 m.

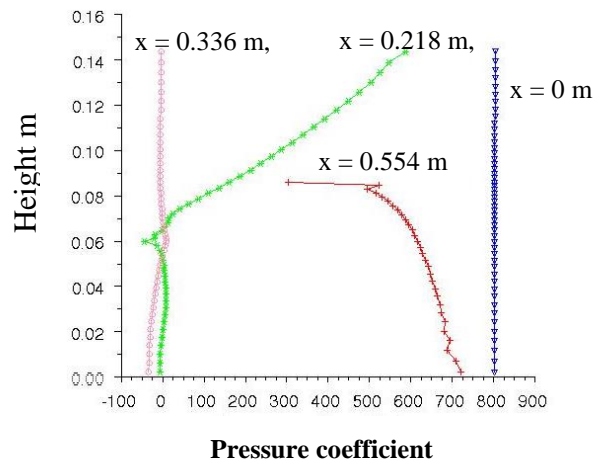


Figure 9. Pressure coefficient at the first plate, second plate, inlet section and outlet section of the duct with obstruction height 0.059 m.

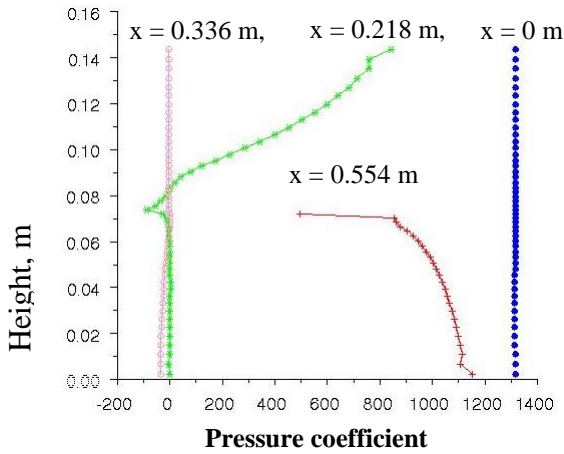


Figure 10. Pressure coefficient at the first plate, second plate, inlet section and outlet section of the duct with obstruction height 0.073 m.

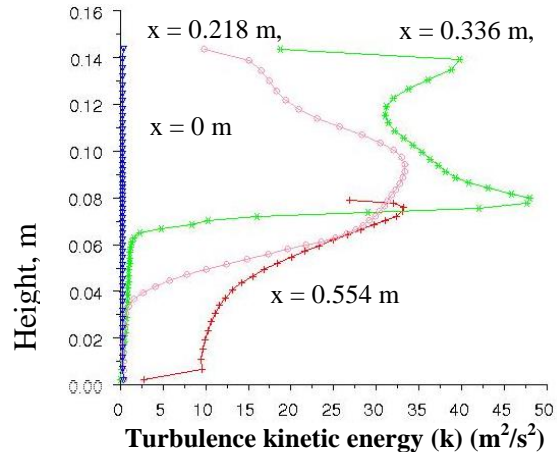


Figure 13. Turbulence kinetic energy at the first plate, second plate, inlet section and outlet section of the duct obstruction height 0.073 m.

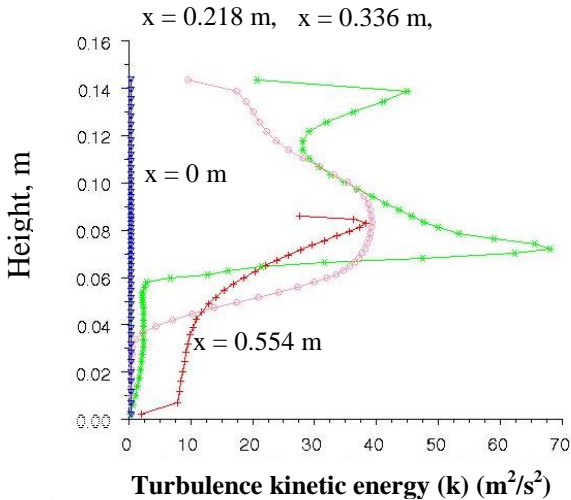


Figure 11. Turbulence kinetic energy at the first plate, second plate, inlet section and outlet section of the duct with obstruction height 0.059 m

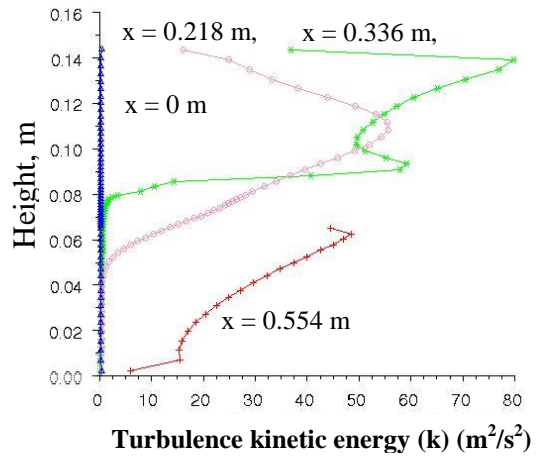


Figure 14. Turbulence kinetic energy at the first plate, second plate, inlet section and outlet section of the duct obstruction height 0.080 m.

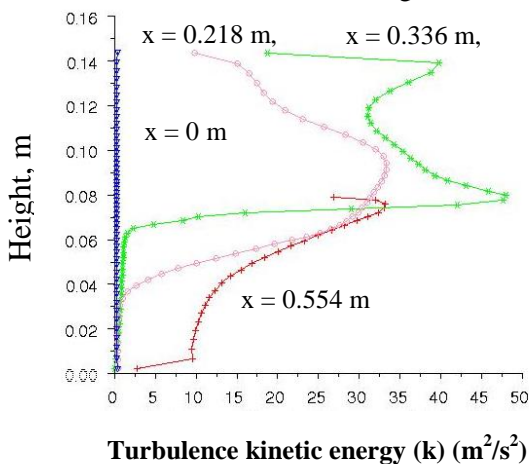


Figure 12. Turbulence kinetic energy at the first plate, second plate, inlet section and outlet section of the duct with obstruction height 0.066 m.

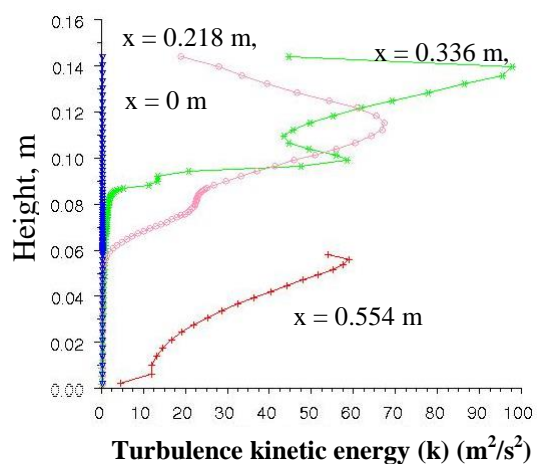


Figure 15. Turbulence kinetic energy at the first plate, second plate, inlet section and outlet section of the duct with obstruction height 0.087 m.

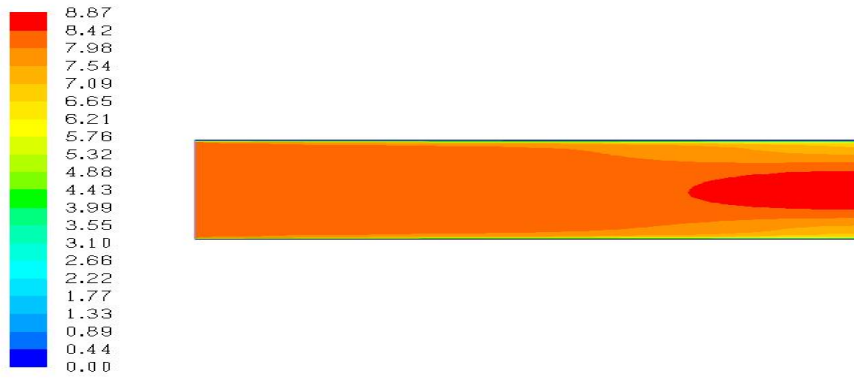


Figure 16. Velocity field distribution in rectangular duct without obstruction plates flow is from left to right, velocity values in (m/s).

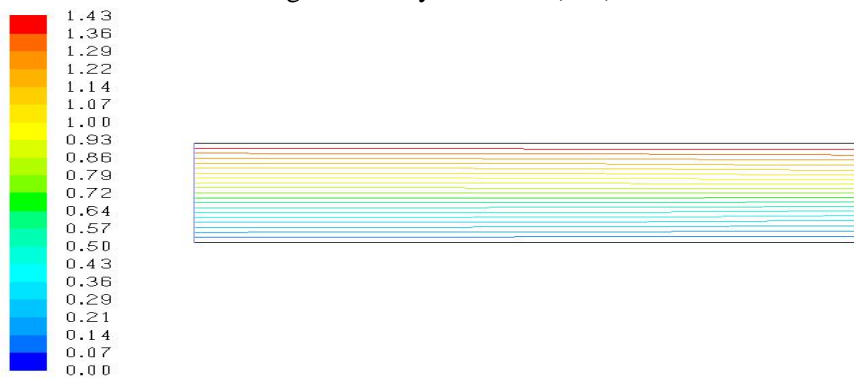


Figure 17. Contours of streamline function distribution in rectangular duct without obstruction plates, flow is from left to right, streamline values in (kg/s).

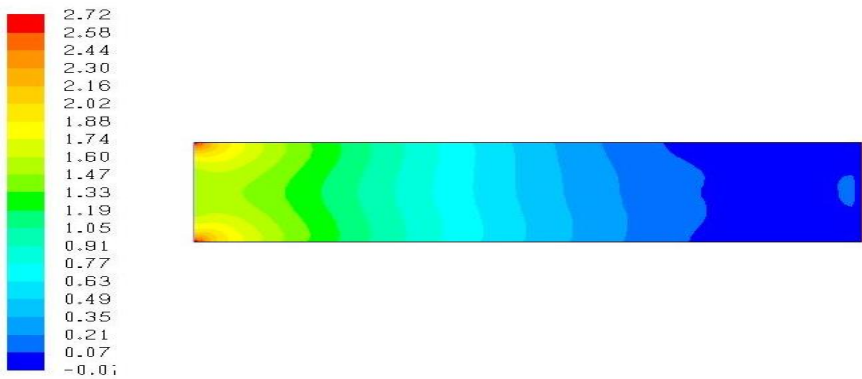


Figure 18. Pressure field distribution in rectangular duct without obstruction plates flow is from left to right, pressure values in (pa).

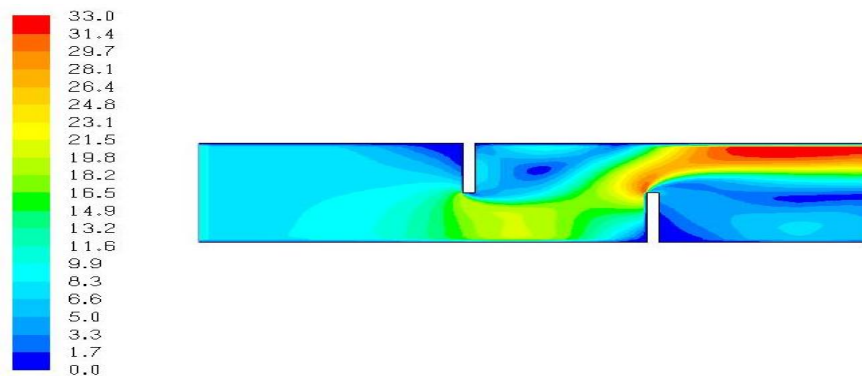


Figure 19. Velocity field distribution. in rectangular duct with obstruction plates height (0.059 m) flow is from left to right, velocity values in (m/s).

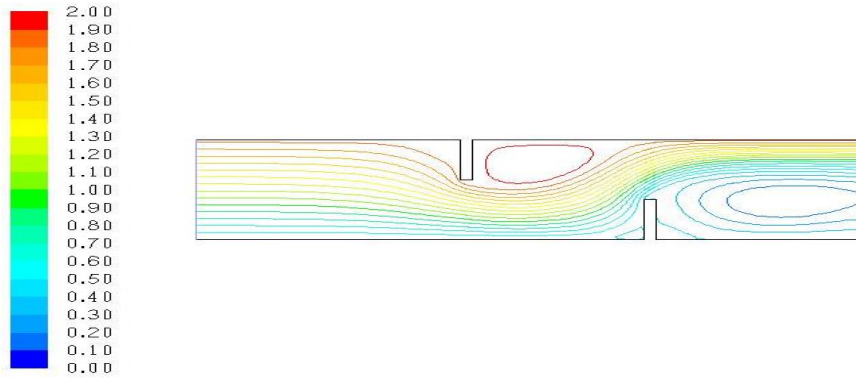


Figure 20. Contores of streamline function distribution. in rectangular duct with obstruction plates height (0.059 m) flow is from left to right, streamline values in (kg/sec).

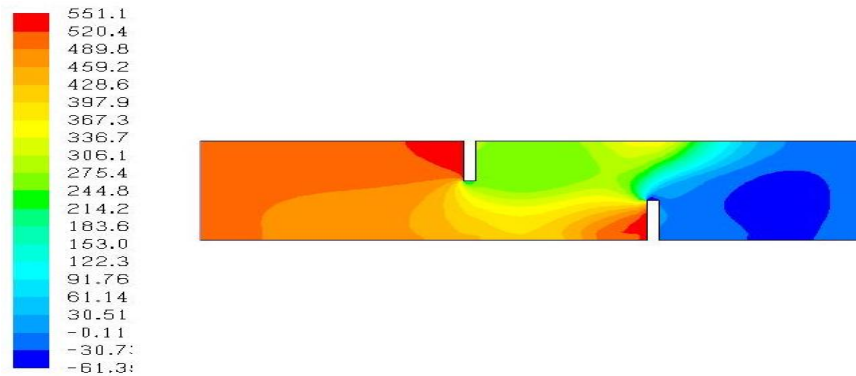


Figure 21. Pressure field distribution in rectangular duct with obstruction plates height (0.059 m) flow is from left to right, pressure values in (pa).

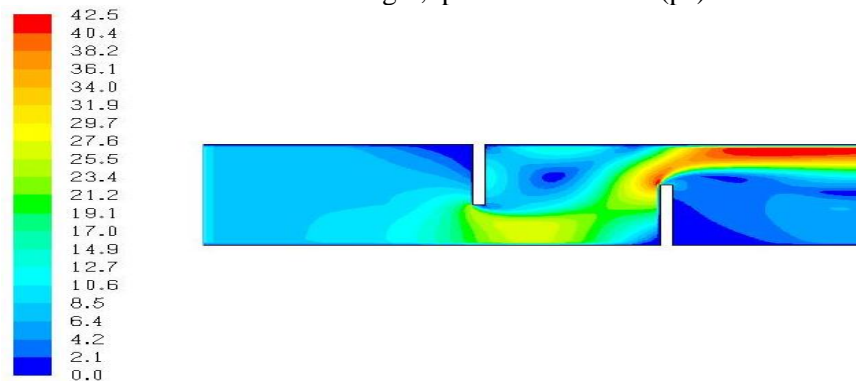


Figure 22. Velocity field distribution in rectangular duct with obstruction plates height (0.087 m) flow is from left to right, Velocity values in (m/s).

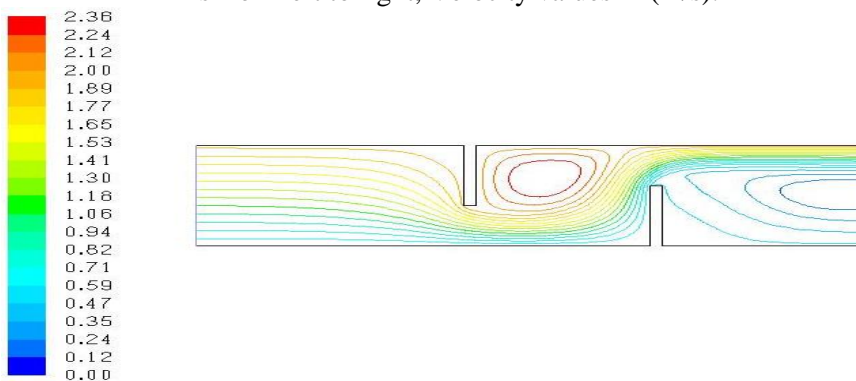


Figure 23. Contores of streamline function distribution in rectangular duct with obstruction plates height (0.087 m) , flow is from left to right, streamline values in (kg/sec)

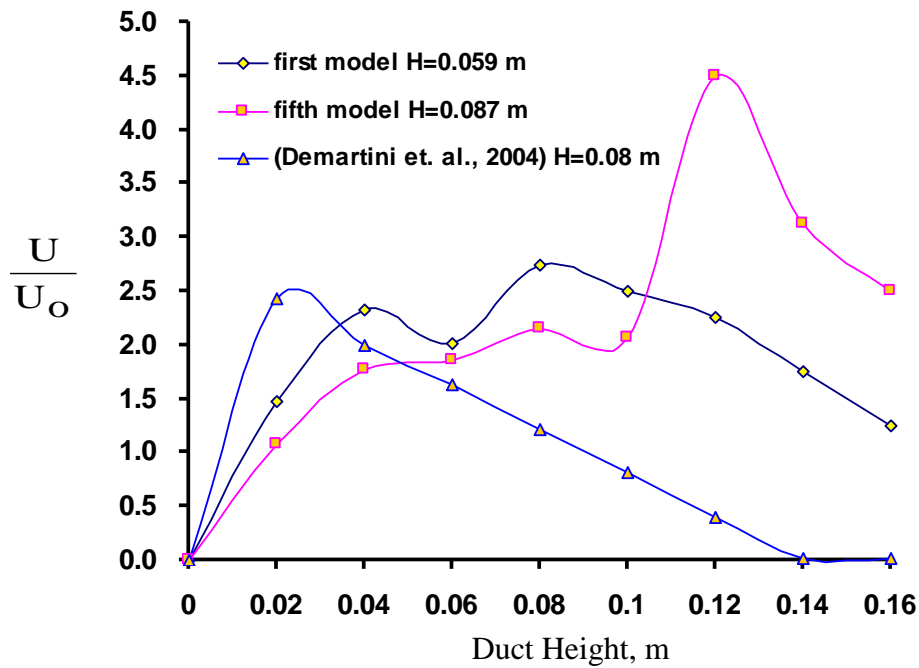


Figure 24. Dimensionless velocity profiles the first obstruction plates ($x=0.218$ m) for the first ($H=0.059$) and fifth model ($H=0.087$) compared with the experimental model of (Demartini et. al., 2004) baffle height ($H=0.08$ m).

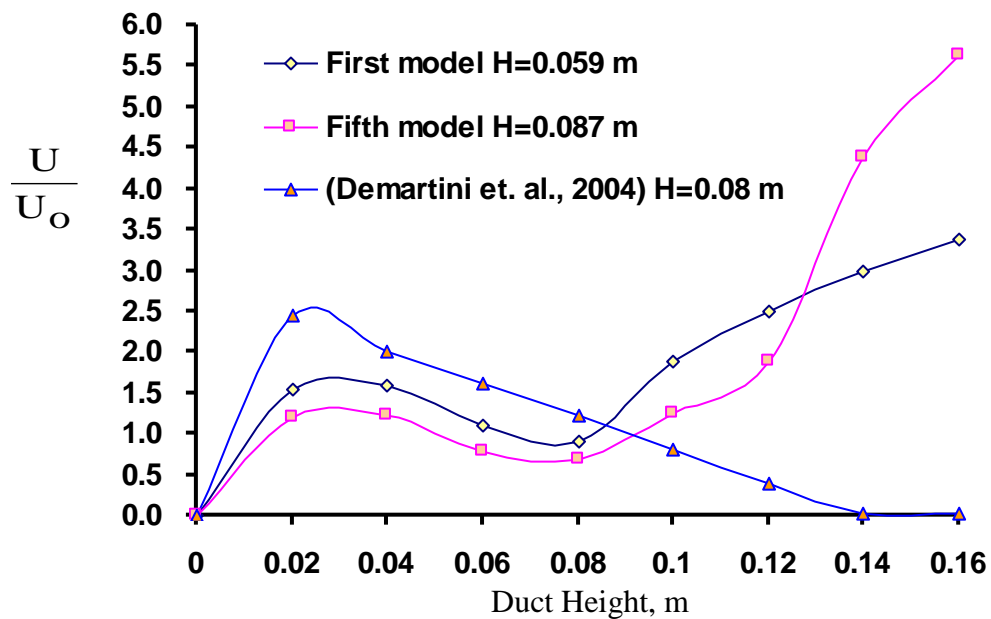


Figure 25. Dimensionless velocity profiles the second obstruction plates ($x=0.336$ m) for the first ($H=0.059$) and fifth model ($H=0.087$) compared with the experimental model of (Demartini et. al., 2004) baffle height ($H=0.08$ m).